

## Response to AMT Reviewer #2

We thank the reviewer for their helpful comments, which have helped to improve the manuscript. Our point-by-point responses are provided below in blue font, with new text added to the manuscript given in italics. Line numbers refer to the new clean version of the manuscript.

The paper "Retrieval of NO<sub>2</sub> profiles from three years of Pandora MAX-DOAS measurements in Toronto, Canada" by Ramina Alwarda et al., presents investigations on the NO<sub>2</sub> profiles retrievals from the offaxis measurement scheme of the Toronto Pandora instrument over 3 years (2018-2020). The retrieval is done using Optimal Estimation HeiPro profiling algorithm and comparing the obtained profiles and partial columns to official Pandora direct-sun measurements, in situ observations, satellite data, and an air quality forecasting model.

The authors find that the HeiPro surface NO<sub>2</sub> are close to the in-situ NAPS measurements (small under-estimation of less than 10%) and underestimating the GEM-MACH model surface value (up to 40%). The HeiPro partial columns (up to 4km) are larger than the satellite S5p data (in agreement to other validation studies), while they are much larger than the direct-sun tropospheric estimate and from the GEM-MACH model.

The paper is interesting, in the scope of AMT, and I would suggest its publication after some revision.

In the current state of the manuscript, a comparison between different datasets is shown, but it is never clear if one of those datasets is considered as a reference, if it has already been validated elsewhere or if it is also prone to (large) uncertainties. The error are never mentioned, so it is not clear if the differences found between the datasets are within the combined uncertainties.

- The biases (both the multiplicative and mean relative) reported in the manuscript all include uncertainties based on the errors of each dataset. For example, the mean relative bias of HeiPro (0–4 km) partial columns to Pandora-DS tropospheric NO<sub>2</sub> is reported as  $61\% \pm 9.7\%$ . Therefore, even when considering the errors, there is a clear positive bias between HeiPro and Pandora-DS. Additionally, the Pandora-DS and TROPOMI tropospheric NO<sub>2</sub> data used in the study have been the subjects of previous air quality studies (e.g., Zhao et al., 2019; Zhao et al., 2022) and so we consider them as 'established' datasets. On the other hand, the HeiPro NO<sub>2</sub> dataset at this measurement site has not been previously studied or published. We have added Table 1 to the manuscript which outlines the key attributes of each dataset, including uncertainties. The table is copied below for reference.

**Table 1. Overview of the key attributes of the NO<sub>2</sub> datasets used in this study.**

| Dataset                                       | Temporal resolution | Horizontal resolution  | Errors/uncertainties  |
|---|---------------------|--|---|
| <b>Pandora-DS total column NO<sub>2</sub></b> | 90 s                | < 4 km (for SZA < 50°)<br>4–17 km (for SZA 50°–80°)<br>(Herman et al., 2009) | 1.3×10 <sup>15</sup> molec/cm <sup>2</sup><br>(Herman et al., 2009, 2018) |
| <b>OMI stratospheric NO<sub>2</sub></b>       | 1 day               | 13 km × 24 km<br>(Krotkov et al., 2017)                                      | 2×10 <sup>14</sup> molec/cm <sup>2</sup><br>(Krotkov et al., 2017)        |
| <b>HeiPro</b>                                 | 22 minutes          | 5–10 km (effective pathlength, Ortega et al., 2015)                          | 4.4×10 <sup>14</sup> molec/cm <sup>2</sup><br>(this work)                 |
| <b>TROPOMI tropospheric NO<sub>2</sub></b>    | 1 day               | 7 km × 3.5 km<br>(5.5 km × 3.5 km since Aug. 2019)                           | 8.5×10 <sup>14</sup> molec/cm <sup>2</sup><br>(Eskes and Eichmann, 2019)  |
| <b>GEM-MACH</b>                               | 1 hour              | 10 km × 10 km  | N/A   |
| <b>In situ NO<sub>2</sub></b>                 | 1 minute            | Point measurement  | 0.4 ppbv<br>(Thermo Scientific, 2015)                                     |

Another point is that a long investigation is performed to try to understand/quantify the causes of the differences between the Pandora MAX-DOAS and the Pandora direct-sun tropospheric estimation, like investigating the influence of the PBL or the impact of different viewing angle due to the NO<sub>2</sub> spatiotemporal heterogeneity but the impact of some more basic assumptions are not really estimated and only very quickly discussed in the conclusion. In my opinion, two points are too briefly mentioned and not quantified enough:

- the choice of MAXDOAS long UV scans (only discussed for the surface results)
- the quality of the Pandora direct-sun tropospheric estimation

We agree that the above two points are briefly mentioned. Please see below our more detailed explanations as to why we believe they are not significantly contributing to the observed biases.

- How would the comparisons for the partial columns be with the long VIS scans?
  - Please see below a plot for partial column comparisons between HeiPro long UV versus long vis as well as a [table](#) (now Table A1 in the Appendix) that summarizes the biases for HeiPro long vis and long UV versus partial columns from Pandora-DS, GEM-MACH, and TROPOMI. As shown in the figure and table, the results and biases are quite similar: (i) the scatter plot below shows a zero-intercept slope of  $0.97 \pm 0.004$  and mean relative bias of  $0.7\% \pm 5.9\%$ , indicating minimal differences between the long UV and long vis partial columns, and (ii) the table below shows that the HeiPro long UV and long vis biases towards the partial columns are quite similar (mostly the same within uncertainties). We now state in the manuscript the following on lines 422–431:

Although the direct-Sun and MAX-DOAS retrieval wavelength ranges are different due to the varying standard protocols for each, it is worthwhile to note that the HeiPro long vis versus long UV NO<sub>2</sub> partial column comparisons showed good agreement with one another, with a zero-intercept slope of  $0.97 \pm 0.004$  and mean relative bias of  $0.7\% \pm 5.9\%$ . We therefore do not expect the choice of retrieval window to significantly impact the HeiPro long UV partial column comparisons to Pandora-DS (see Table A1 below for the HeiPro long vis partial column NO<sub>2</sub> comparisons).

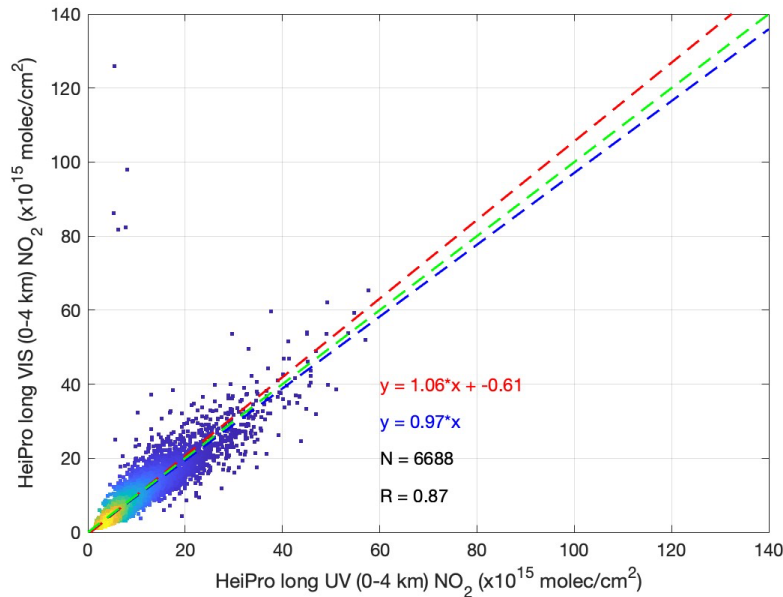


Figure above (not in main manuscript or Appendix) shows the 0–4 km NO<sub>2</sub> column comparisons for HeiPro long vis vs. long UV.

Table A1. Multiplicative and mean relative biases ( $\pm$  uncertainties) of HeiPro towards NO<sub>2</sub> partial columns from Pandora-DS, TROPOMI, and GEM-MACH, for both the HeiPro long UV and long vis results.

| NO <sub>2</sub> Partial Column Comparison |                     | HeiPro Scan Type |                |
|---|---------------------|------------------|----------------|
|   |                     | long UV          | long vis       |
| HeiPro vs. Pandora-DS partial columns     | Multiplicative Bias | 51% $\pm$ 0.8%   | 49% $\pm$ 0.9% |
|   | Mean Relative Bias  | 61% $\pm$ 9.7%   | 61% $\pm$ 6.8% |
| HeiPro vs. TROPOMI                        | Multiplicative Bias | 17% $\pm$ 4.0%   | 13% $\pm$ 4.6% |
|   | Mean Relative Bias  | 37% $\pm$ 51%    | 40% $\pm$ 45%  |
| HeiPro vs. GEM-MACH                       | Multiplicative Bias | 12% $\pm$ 1.2%   | 13% $\pm$ 1.3% |
|   | Mean Relative Bias  | 67% $\pm$ 7.1%   | 64% $\pm$ 2.4% |

- How is the HeiPro MAX-DOAS comparing to the direct-sun total NO<sub>2</sub> data?

- We now include the figure below in the Appendix (Figure A4). Panel (a) shows the MAX-DOAS HeiPro comparisons to Pandora-DS total column NO<sub>2</sub>. As expected, due to the larger

Pandora-DS columns now being compared, the bias is much lower ( $16\% \pm 0.69\%$  multiplicative bias and  $6.1\% \pm 4.8\%$  mean relative bias). We now state the following in the manuscript on lines 461–464:

*For reference, HeiPro (0–4 km) vs. Pandora-DS total columns are compared in panel (a) of Fig. A4, which shows that HeiPro partial columns exhibit a positive multiplicative bias of  $16\% \pm 0.7\%$  and a mean relative bias of  $6.1\% \pm 4.8\%$ . Not surprisingly, there is better agreement here as compared to Fig. 3a (i.e., HeiPro vs. Pandora-DS tropospheric NO<sub>2</sub>) since the Pandora-DS total columns are larger.*

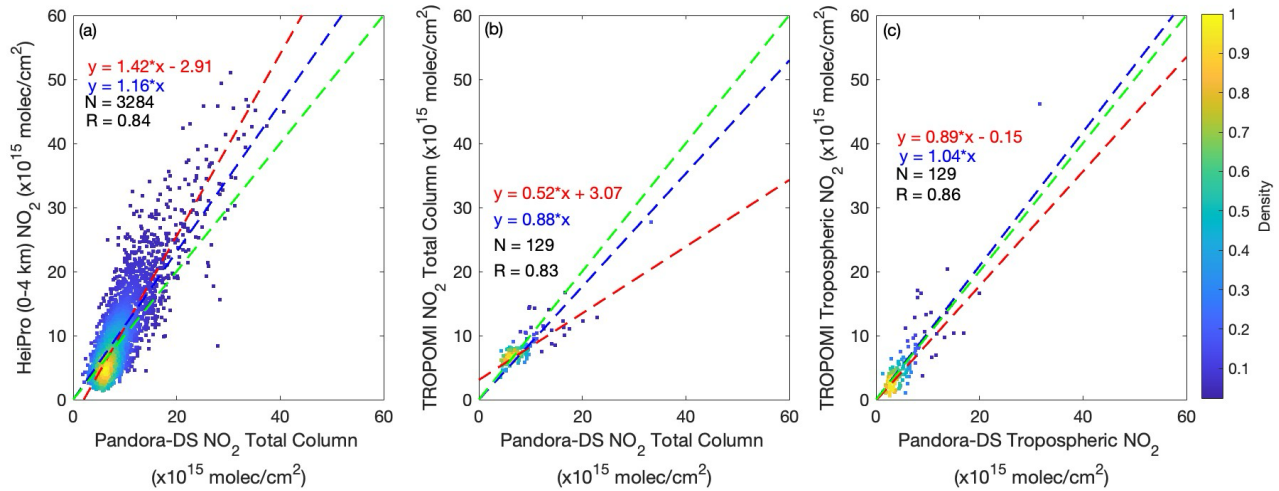


**Figure A4. Comparisons (2018–2020) of (a) HeiPro (0–4 km) NO<sub>2</sub> partial columns vs. Pandora-DS NO<sub>2</sub> total columns, (b) TROPOMI vs. Pandora-DS NO<sub>2</sub> total columns, and (c) TROPOMI vs. Pandora-DS tropospheric NO<sub>2</sub> columns. The dashed lines and color bar are as indicated in Fig. 3.**

- how much is removed from the original direct-sun total NO<sub>2</sub> dataset to create the tropospheric dataset?

- The stratospheric NO<sub>2</sub> that is removed represents  $34\% \pm 2.8\%$  of the original Pandora direct-Sun total column NO<sub>2</sub> (this percentage is both the mean & median value). The following text has been added to the manuscript on lines 215–216:  
*The stratospheric portion that was removed accounted for  $34\% \pm 2.8\%$  of the Pandora-DS NO<sub>2</sub> total columns.*
- To get another estimate of the stratospheric-to-total column ratio at this measurement site, we use TROPOMI data (version 2.3.1) from 2018–2020 with a qa\_value  $\geq 0.75$ , within 10 km of the measurement site and 10 minutes of the Pandora-DS measurement time. The stratospheric-to-total column ratio is  $44\% \pm 9.7\%$ , which is within the uncertainty of  $34\% \pm 2.8\%$ , the amount of NO<sub>2</sub> removed using the Prtmo-OMI method. Please note that the stratospheric portion reported using TROPOMI is only during the satellite overpass time (13:30 LT), but we do not expect this value to change drastically if we were to incorporate data points across the entire day.

- how good is the OMI stratospheric estimation? and its diurnal evolution estimation from the model?

- The OMI stratospheric NO<sub>2</sub> data product we are using (version 3, Krotkov et al., 2017) has been used in previous publications (e.g., Choi et al., 2020, Zhao et al., 2022) and has been validated with satellite and ground-based instruments (Krotkov et al., 2017). Panel (c) of [Figure A4](#) shows good agreement between TROPOMI and Pandora-DS tropospheric NO<sub>2</sub> (multiplicative bias:  $-4.4\% \pm 3.5\%$  ; mean relative bias:  $-0.9\% \pm 34\%$ ), indicating a reasonable stratospheric estimation at the measurement site in this study. The diurnal evolution estimation from the Pratmo model has been used previously in Zhao et al. (2019). More details of the performance of this method can be found in their Appendix B.

- how do the original direct-sun total NO<sub>2</sub> compare to S5p total NO<sub>2</sub>?

- [Figure A4](#) in the Appendix (shown above) now includes comparisons between Pandora-DS and TROPOMI total column NO<sub>2</sub> in panel (b) and tropospheric NO<sub>2</sub> in column (c). We now state in the manuscript the following on lines 461–475:

*The TROPOMI vs. Pandora-DS NO<sub>2</sub> total and tropospheric column comparisons are shown in Fig. A4b–c, respectively. Pandora-DS and TROPOMI show good agreement with one another for both total column (multiplicative bias:  $-12\% \pm 1.9\%$ ; mean relative bias:  $0.1\% \pm 21\%$ ) and tropospheric NO<sub>2</sub> (multiplicative bias:  $-4.4\% \pm 3.5\%$  ; mean relative bias:  $-0.9\% \pm 34\%$ ). Note that the large uncertainties are due to the relatively large TROPOMI total column and tropospheric NO<sub>2</sub> errors. Additionally, the tropospheric NO<sub>2</sub> agreement in panel (c) provides more confidence in the stratospheric-tropospheric separation method that was used in the study (i.e., Pratmo-OMI data). TROPOMI total column NO<sub>2</sub> at this measurement site has been studied and validated in Zhao et al. (2020). Using the version 1 data product, Zhao et al. (2020) found that TROPOMI vs. Pandora-DS total column NO<sub>2</sub> had a zero-intercept slope of 0.70 and correlation coefficient of 0.75. The version 2.3 data product used in this work showed an improvement from version 1, with a zero-intercept slope of 0.89 and correlation coefficient of 0.81. The time period of the study in which version 1 was used (March 2018 to March 2019) was similar to that of this study (May 2018 to June 2020). Comparisons and validation of the newer version 2.3 TROPOMI data products are outside the scope of this work.*

These quantifications would allow to have more confidence in the Pandora retrievals and put the HeiPro data in relation to some reference data.

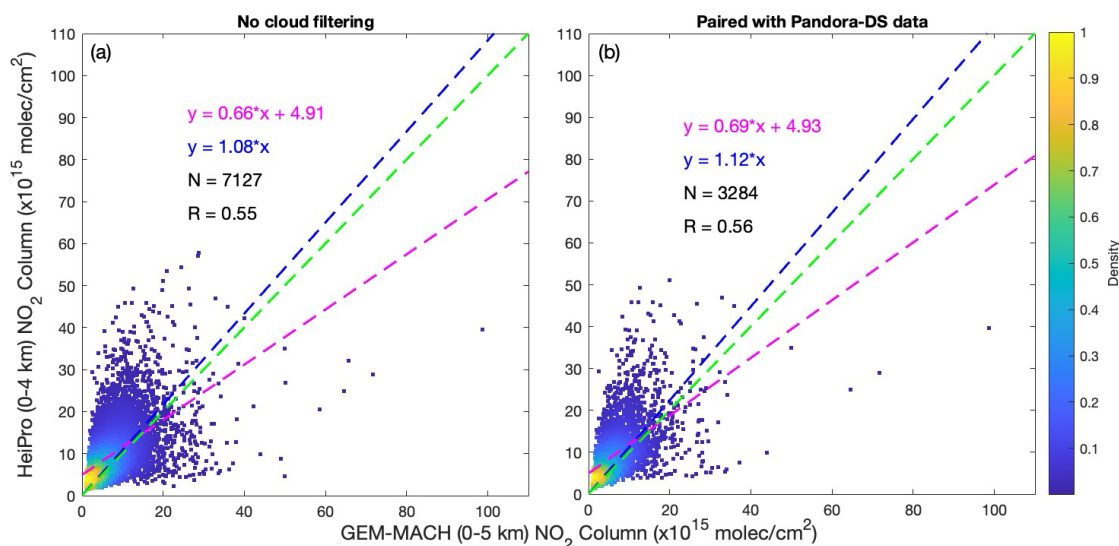
The summary in my understanding:

1) HeiPRO VCD (0-4km) are larger than: a) PGN-DStropo (by a lot!), b) S5p (by a quantity similar to what other validation in similar context has found), c) the GEM-MACH model. For the latter case, it is clear in Fig4 (although the larger differences are in winter months where maybe the number of points is not so representative?), but in Fig3c the comparison is more scattered and less clear.

- For the latter case (i.e., HeiPro vs. GEM-MACH), we believe that there is still a sufficient number of data points in winter months:  $N_{\text{spring}} = 1827$ ;  $N_{\text{summer}} = 2657$ ;  $N_{\text{fall}} = 1574$ ;  $N_{\text{winter}} = 646$ .

The first 2 cases imply clear-sky conditions (direct-sun measurements for one, and some cloud filtering for the satellite pixels in the second case). Are the comparisons wrt model done with some kind of filtering too (ie cloud filtering)? is not, would this improve the comparison? Maybe you could try to see if the comparisons with the model improves if you only select the same comparisons pairs that are selected when comparing HeiPRO to the direct-sun (ie the clear sky cases)?

- Thank-you for this interesting suggestion. There was no cloud filtering done with the HeiPro vs. GEM-MACH comparisons. Although we do not have any cloud filtering/flags in the GEM-MACH data, we paired the GEM-MACH data with the HeiPro – Pandora-DS dataset, which would effectively ensure that GEM-MACH is now being compared to HeiPro under clear-sky conditions. The figure below shows the resulting comparison: the left panel is the original (as-is in the manuscript) while the right panel is the “clear-sky” case: there is only a small difference (panel (a) has a zero-intercept slope of 1.08 and mean relative bias of  $60\% \pm 7.5\%$ , panel (b) has a zero-intercept slope of 1.12 and mean relative bias of  $67\% \pm 7.1\%$ ). Please note that because the HeiPro and Pandora-DS data are hourly averages, merging them with the GEM-MACH data does not fully ensure a clear-sky comparison since there may still be both clear and cloudy skies within one hour of measurements. In the manuscript, we have replotted Fig. 3a and 3c to show only the coincident data among HeiPro, Pandora-DS, and GEM-MACH, and so panel (b) below has replaced Fig. 3c.



Comparisons between HeiPro (0–4 km) NO<sub>2</sub> partial columns (2018–2020) vs. (a) GEM-MACH (0–5 km) partial columns and (b) GEM-MACH (0–5 km) partial columns paired with Pandora-DS data. The zero-intercept linear regression (dashed blue line), ordinary least squares regression (dashed magenta line), and the 1:1 line (dashed green line) are depicted. The color bar indicates the normalized density of the data points. Figure not shown in main manuscript or Appendix.

2) Heipro surface concentration are smaller than: a) NAPS (by 4.4%/9%), b) model (by 40% and 36%)

When the model is smoothed with the MAX-DOAS AVK, the agreement seems better. We only see it in Fig.8. Please give numbers for this case too, as it seems important to me to report on the differences when taking into account the vertical sensitivity of each technique.

- In the manuscript, we now state the following on lines 837–846:  
*Across all seasons, the HeiPro NO<sub>2</sub> median profiles from 0–200 m underestimate the unsmoothed GEM-MACH median values, while from 1.5–4 km, the HeiPro median profiles then overestimate the unsmoothed GEM-MACH median values. For the 0–200 m layer, the mean relative bias of HeiPro towards GEM-MACH decreases from –37% (unsmoothed) to –6.1% (smoothed). Note that these biases are representative of the integrated 0–200 m layer and may differ slightly from the surface values reported in Table 2. The most significant changes occur in the layer from 1.5–4 km, where the HeiPro bias towards GEM-MACH decreases from > 1000% (unsmoothed) to 2.6% (smoothed). The HeiPro surface underestimation and free tropospheric overestimation of the unsmoothed GEM-MACH profiles can probably be explained by the NO<sub>2</sub> inventories used in the GEM-MACH model, which, respectively, (i) utilize older inventories that do not account for reduced emissions over the years, and (ii) do not account for free tropospheric NO<sub>2</sub> sources while the a priori NO<sub>2</sub> profile contains free tropospheric NO<sub>2</sub>.*

It would be good to add a table with the summary differences for all the cases.

- Thank-you for this suggestion. In the Conclusions section, we have added Table 2 (copied below for reference), which summarizes the biases for all the partial column and surface NO<sub>2</sub> intercomparisons presented in this work.

**Table 2. Summary of the multiplicative biases and mean relative biases ( $\pm$  uncertainties) for the HeiPro comparisons to partial columns and surface NO<sub>2</sub>.**

| Datasets compared   | Multiplicative Bias (%) | Mean Relative Bias (%) |
|---|-------------------------|------------------------|
| HeiPro (0-4 km) vs. Pandora-DS tropospheric NO <sub>2</sub> | 51% $\pm$ 0.8%          | 61% $\pm$ 9.7%         |
| HeiPro (0-4 km) vs. TROPOMI tropospheric NO <sub>2</sub>    | 17% $\pm$ 4.0%          | 37% $\pm$ 51%          |
| HeiPro (0-4 km) vs. GEM-MACH (0-5 km) NO <sub>2</sub>       | 12% $\pm$ 1.2%          | 67% $\pm$ 7.1%         |
| HeiPro vs. NAPS in situ surface NO <sub>2</sub>             | –5.8% $\pm$ 0.7%        | –9.7% $\pm$ 7.5%       |
| HeiPro vs. GEM-MACH surface NO <sub>2</sub>                 | –41% $\pm$ 0.5%         | –37% $\pm$ 2.4%        |
| HeiPro vs. GEM-MACH-smoothed surface NO <sub>2</sub>        | –30% $\pm$ 0.8%         | –6.0% $\pm$ 3.4%       |

detailed comments:

-----

- line 88-89: "Comparisons of these PGN sky algorithm data products with other datasets at the measurement site in this study will be the subject of a future study" --> this is a pity that is not included here, it would have brought an interesting additional comparison.

- We agree that the inclusion of the PGN sky algorithm data products would have been an interesting additional comparison. However, current PGN sky data products are produced using the vis band fitting algorithm, not yet available for UV NO<sub>2</sub>. We are working with PGN on a detailed validation and verification of UV NO<sub>2</sub> sky algorithm data products. But this is beyond the scope of current work (to validate the optimal-estimated-based retrieval).

- Fig1: I would move this figure when explaining the differences in pointing between the MAX-DOAS and the direct-sun. Also add in the caption what time-period has been averaged to create the S5p NO<sub>2</sub> map.

- Figure 1 has now been moved to Section 2. The time period (2018–2020) was previously mentioned, but we have now specified which months (May 2018 – December 2020).

- line 194-> 197: the explanation of the stratospheric estimation subtraction is presented here too quickly, and then again mentioned in Sect. 2.3.1. I would suggest to have one section explaining this part, with an illustration of the outcome and some quantification of the errors related to this step. When reading this part now, I have many questions coming up: why OMI and not S5p? and why that OMI product? is there any reference showing that it is a good stratospheric dataset? has it been validated?

- TROPOMI was not used to remove the stratospheric portion because we wanted to use an independent stratospheric data product that was not a part of the partial column intercomparisons. Additionally, according to Krotkov et al. (2017), the OMI stratospheric data product we used (v3) shows good agreement with the verification algorithm used for TROPOMI. Compared to v2 of the OMI stratospheric data product, v3 shows a reduced bias towards other satellite and ground-based datasets (Krotkov et al., 2017). Furthermore, this stratospheric NO<sub>2</sub> data product has been used in previous publications (e.g., Choi et al., 2020, Zhao et al., 2022) and has been validated with satellite and ground-based instruments. Lastly, as seen in [Figure A4c](#), TROPOMI vs. Pandora-DS tropospheric NO<sub>2</sub> shows good agreement, providing further support for the Prtmo-OMI stratospheric-tropospheric separation method used in this study.

-For my own curiosity: are you performing zenith-sky twilight measurements with the Pandora? if yes, you could also derive some stratospheric NO<sub>2</sub> estimation from the Pandora itself...

- The Pandora does make zenith-sky twilight measurements. We will keep this suggestion in mind for future studies using stratospheric NO<sub>2</sub> at the measurement site.

- Pandora DS: I think it would be good to show its coherence wrt S5p total NO<sub>2</sub> (eventually in the annex) - and discuss that this was done in the past, ie Zhao et al 2020, although with a previous/different S5p product version.

- We now include [Figure A4](#) in the Appendix, with Figure A4b showing the TROPOMI vs. Pandora-DS total column NO<sub>2</sub> comparisons. We also state the following on lines 469–475: *TROPOMI total column NO<sub>2</sub> at this measurement site has been studied and validated in Zhao et al. (2020). Using the version 1 data product, Zhao et al. (2020) found that TROPOMI vs. Pandora-DS total column NO<sub>2</sub> had a zero-intercept slope of 0.70 and*



*correlation coefficient of 0.75. The version 2.3 data product used in this work showed an improvement from version 1, with a zero-intercept slope of 0.89 and correlation coefficient of 0.81. The time period of the study in which version 1 was used (March 2018 to March 2019) was similar to that of this study (May 2018 to June 2020). Comparisons and validation of the newer version 2.3 TROPOMI data products are outside the scope of this work.*

- Sect. 2.2.2: explain a bit more the DOF from MAXDOAS, show an AVK and discuss more/show more results from both UV and VIS channel of the MAX-DOAS (not only decide because the long UV are in a closer agreement with the surface NAPS. By the way, I am not totally convinced by this statement. You base your analysis on the fact that the multiplicative factor in Fig A2a) is smaller than in A2b). But the regression slope and intercepts are smaller for A2b) than for A2a)...

- To expand on the DOFS discussion, the following text has been added to the manuscript on lines 314–315:  
*...the degrees of freedom for signal (DOFS) for each profile, which represents the number of independent pieces of information obtained from the measurements...*
- We have additionally added the following text to the manuscript on lines 327–331:  
*Lastly, retrievals for which both the NO<sub>2</sub> profiles and aerosol extinction profiles had DOFS < 1 were excluded from the analysis for quality control purposes (e.g., Vlemmix et al., 2015) and represented 19% of the dataset. Such retrievals contain limited information from the measurements and are more influenced by the a priori profile. The mean DOFS values before and after filtering are  $1.61 \pm 0.68$  and  $1.88 \pm 0.42$  for aerosol extinction, respectively, and  $2.35 \pm 0.49$  and  $2.39 \pm 0.40$  for NO<sub>2</sub>, respectively.*
- Regarding results from both MAX-DOAS UV and vis channels, we have added [Table A1](#) to the Appendix, which summarizes the biases of HeiPro long UV versus NO<sub>2</sub> partial column comparisons as well as long vis versus NO<sub>2</sub> partial column comparisons.
- Regarding the averaging kernels, we have added Fig. A3 to the Appendix (copied below for reference), which displays averaging kernels for both NO<sub>2</sub> and aerosol extinction profile retrievals that meet the DOFS threshold, along with the respective dSCDs of NO<sub>2</sub> and O<sub>4</sub>.

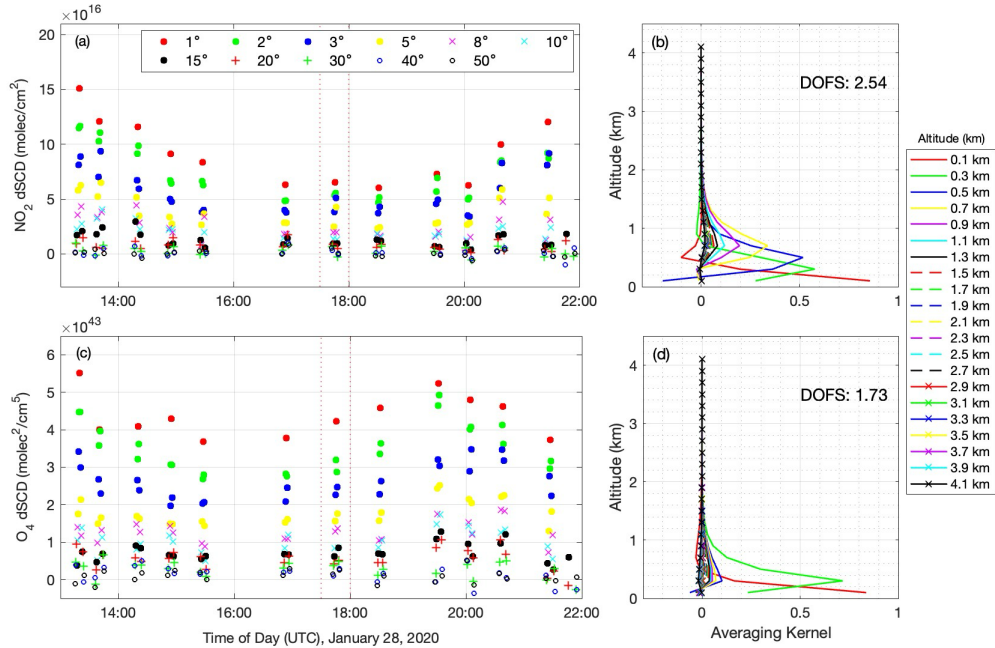


**Figure A3: MAX-DOAS dSCDs (UV, 338–370 nm) of (a)  $\text{NO}_2$  and (c)  $\text{O}_4$  retrieved on January 28, 2020. The right panels show the averaging kernels and respective DOFS for a single HeiPro profile retrieval of (b)  $\text{NO}_2$  and (d) aerosol extinction. The dSCDs used in the  $\text{NO}_2$  and aerosol extinction profile retrievals are indicated by the red dashed lines in panels (a) and (c), respectively.**

- Regarding the regression slope and intercept for Figure A2a (long UV) vs. A2c (long vis), we identified that there was a small bug in the code whereby the long vis scans were being plotted as the short UV and vice versa. The corrected figure (Fig. A2) is now in the manuscript and is added below for reference. Long vis scans show larger slopes for both regressions and a larger intercept as well as a lower R value compared to the long UV. We have added the following text in the manuscript on lines 319–320:  
*Lastly, the long UV scans show improved regression slopes, intercept, and correlation coefficient to the NAPS in situ surface VMRs compared to the long vis scans (see Fig. A2).*

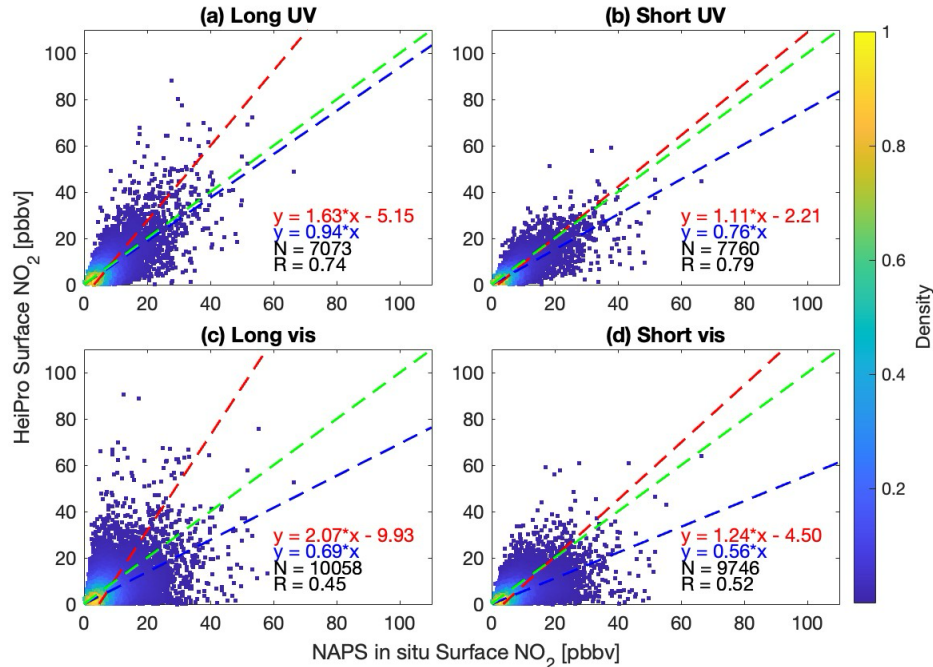


**Figure A2. Scatter plots for HeiPro surface NO<sub>2</sub> vs. NAPS in situ surface NO<sub>2</sub> VMRs for scan types and retrieval windows of (a) long UV, (b) short UV, (c) long vis, and (d) short vis. Only the long UV scans were incorporated in the results of this work. The dashed lines and color bar are as indicated in Fig. 3.**

Please also double check numbers. They are different in Fig A2a) and in in Fig 6a), while in my understanding, they are presenting the same datasets...

- The reason for the differences is because in Fig. 6a, the data points ( $N=6950$ ) represent coincident data points among NAPS in situ, HeiPro, and GEM-MACH, while the data points in Fig. A2a ( $N=7322$ ) represent coincident data points between NAPS in situ and HeiPro only. The number of data points in Fig. A2a has changed to  $N=7073$  after fixing a small bug in the code.

- lines 223-215: the choice of only using the long scans make sense to me (more information content with larger number of elevation angles) and is confirmed by the larger DOFs and RMS (not clear what RMS is meant in line 228), but then the choice of using the long UV scans instead of the long VIS scans is less convincing to me. They are more in agreement with the surface NO<sub>2</sub> (with the theory that the horizontal extent of the line-of-sight is smaller, ok), but this reason is not so applicable to the direct-sun Pandora geometry or the satellite and model extent.

- Thank-you for catching the use of "RMS" here. It is not RMS, but the HeiPro retrieved NO<sub>2</sub> partial column errors. We have fixed the axis in Figure A1 and any references in the text to indicate that these are partial column errors (lines 317 and 1018).
- The long UV scans were in closer agreement with the surface NO<sub>2</sub> due to the horizontal extent, while for the partial column comparisons, the biases of HeiPro long UV to the Pandora-DS, TROPOMI, and GEM-MACH partial columns were quite similar to those of HeiPro long vis to Pandora-DS, TROPOMI, and GEM-MACH partial columns. Because of the

similar performance to the partial columns, the agreement with the surface NO<sub>2</sub> became the deciding factor for which NO<sub>2</sub> retrieval window to use.

- I would show or at least comment the difference between results with both UV and VIS retrievals later on in the manuscript (at least as a form of error estimation?).

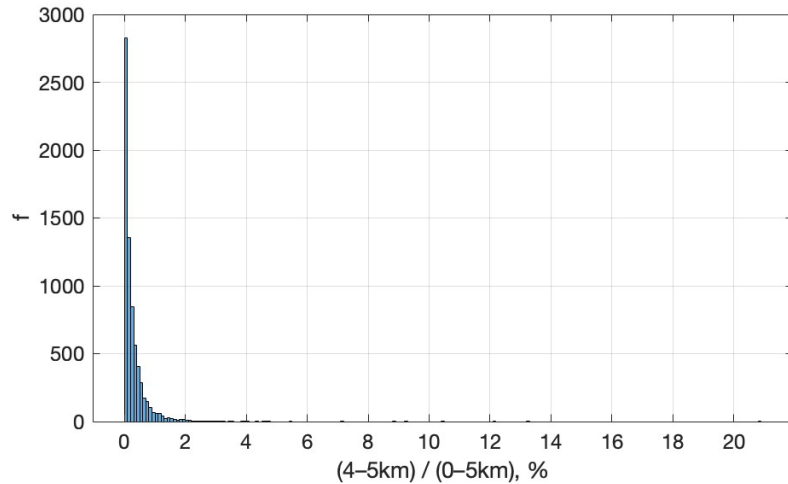
- As shown in the HeiPro long vis versus long UV scatter plot [above](#) and [Table A1](#) immediately following it, there is a minimal difference between results with both long UV and long vis retrievals when comparing partial columns. For the most part, the biases relative to other datasets when using long UV and when using long vis are within the error estimates. We have now included the following in the manuscript (lines 422–431):

*Although the direct-Sun and MAX-DOAS retrieval wavelengths are different due to the varying standard protocols for each, it is worthwhile to note that the HeiPro long vis versus long UV NO<sub>2</sub> partial column comparisons showed good agreement with one another, with a zero-intercept slope of  $0.97 \pm 0.004$  and mean relative bias of  $0.7\% \pm 5.9\%$ . We therefore do not expect the choice of retrieval window to significantly impact the HeiPro long UV partial column comparisons to Pandora-DS (see Table A1 for the HeiPro long vis partial column NO<sub>2</sub> comparisons).*

- line 268: GEM-MACH partial columns 0-5km. If you have the profiles, why you calculate the partial column up to 5km and not 4 km, as the MAX-DOAS?

- The GEM-MACH standard dataset contained NO<sub>2</sub> profiles from 0–5 km and the integrated 0–5 km partial columns. While it makes more sense to only report 0–4 km GEM-MACH columns, this would require a re-integration of the partial columns. This can be done but was avoided because the GEM-MACH NO<sub>2</sub> VMRs from 4–5 km are  $\ll 0.1$  ppbv, with the mean VMR at this altitude range being 0.0188 ppbv. We did a test regarding how much the NO<sub>2</sub> from 4–5 km contributes to the GEM-MACH (0–5 km) NO<sub>2</sub> VCD by integrating the data from 4–5 km and dividing by the (0–5 km) NO<sub>2</sub> VCD. We found this value to be 0.293% (see histogram below). We therefore do not expect that the 0–4 km GEM-MACH columns will vary significantly from the 0–5 km GEM-MACH columns. We have added the following text to the manuscript on lines 672–674:

*While the GEM-MACH standard dataset includes partial columns from 0–5 km, we did not generate a 0–4 km partial column because we found the GEM-MACH NO<sub>2</sub> VMRs from 4–5 km to be very small, and that the integrated NO<sub>2</sub> from 4–5 km constituted only 0.3% of the GEM-MACH (0–5 km) partial columns.*



**Histogram of the frequency of the percent contribution of the 4–5 km GEM-MACH partial column to the 0–5 km GEM-MACH partial column for NO<sub>2</sub> at Downsview. Figure not added to manuscript or Appendix.**

- line 269: are the emissions in the model different for 2018, 2019 and 2020? you say in the discussion/conclusion that the emissions are outdated, and probably too high...

- The anthropogenic emissions used before September 2018 were based on the 2010 Canadian Air Pollutant Emission Inventory (APEI), the 2011 US National Emissions Inventory (NEI), and the 1999 Mexican inventory; after September 2018, the emissions were updated using the 2013 Canadian APEI, the projected 2017 US NEI, and the 2008 Mexican inventory. Given that most emissions have been rapidly trending downwards in both Canada and the US, the statement that the emissions used in GEM-MACH are probably high is correct. For example, the newest GEM-MACH emission dataset, which is based on the projected 2020 Canadian APEI and the projected 2023 US NEI and was implemented operationally in November 2021, has 20% less Canadian NO<sub>x</sub> relative to the previous emissions (and 30% less NO<sub>x</sub> for the US).

- line 281: why you use York linear fit for fig 3a and b) and then switch to ordinary linear regression in fig 3c)? it is a bit confusing

- The ordinary linear regression was used in Fig. 3c because the GEM-MACH data does not have uncertainty estimates. Therefore, a York linear regression could not be used. This has now been stated in the manuscript on lines 413–416:

*Three types of linear regressions are presented in Fig. 3: the first is the York linear fit (York et al., 2004) in which the uncertainties in both datasets are incorporated into the regression, the second is the zero-intercept linear regression, and the third is the ordinary least squares linear regression (used only for the HeiPro vs. GEM-MACH regression since error estimates were not available for GEM-MACH data).*

- fig3: here or in the annex, I would add a plot of HeiPRO vs PGN total direct-sun and of PGN total direct-sun vs S5p total NO<sub>2</sub>.

- Please see the [figure](#) above (added to the Appendix as Fig. A4) which plots (a) HeiPro (0–4 km) vs. Pandora-DS total column NO<sub>2</sub>, (b) TROPOMI vs. Pandora-DS total column NO<sub>2</sub>,

and (c) TROPOMI vs. Pandora-DS tropospheric NO<sub>2</sub>. We have also added the following text to lines 464–469 to discuss and reference this figure:

*The TROPOMI vs. Pandora-DS NO<sub>2</sub> total and tropospheric column comparisons are shown in Fig. A4b–c, respectively. Pandora-DS and TROPOMI show good agreement with one another for both total column (multiplicative bias:  $-12\% \pm 1.9\%$ ; mean relative bias:  $0.1\% \pm 21\%$ ) and tropospheric NO<sub>2</sub> (multiplicative bias:  $-4.4\% \pm 3.5\%$ ; mean relative bias:  $-0.9\% \pm 34\%$ ). Note that the large uncertainties are due to the relatively large TROPOMI total column and tropospheric NO<sub>2</sub> errors. Additionally, the tropospheric NO<sub>2</sub> agreement in panel (c) provides more confidence in the stratospheric-tropospheric separation method that was used in the study (i.e., Prato-OMI data).*

- why not stop the GEM-MACH partial columns 0-5km to 4km for fig 3 c)? as said above, you could integrate the GEM-MACH profiles only up to 4 km, to have the same vertical extent than the MAX-DOAS.

- Please see the [response above](#) as this point was also mentioned earlier.

- line 399: " as well as the different horizontal sensitivities between the direct-Sun and multi-axis viewing geometries." --> you could refer here also to the HeiPRO data retrieved in the VIS long scans, which are sensitive to another (longer) horizontal path ?

- Although the HeiPro long vis data is indeed sensitive to a longer horizontal path, both the long UV and long vis data performed similarly compared to one another and compared to the Pandora-DS tropospheric columns (as shown in [Table A1 above](#)). The differing horizontal sensitivities between the UV and vis do not seem to be able to explain the results since they perform similarly.

- line 574: " this appears to skew the profile shape (see HeiPro profiles near 0 m in Fig. 8)," : I don't understand what your refer to.

- This has been reworded to the following (lines 816–819):  
*When plotting the median profiles, as is done in Fig. 8, it appears as though the extrapolation to the surface does not have a sharper gradient towards the surface (see HeiPro profiles in Fig. 8), although this is only because the median values are plotted; aside from profiles with lofted layers, each individual profile has a larger increase from the 100 m layer to the surface.*

- line 590: "do not account for free tropospheric NO<sub>2</sub> sources while HeiPro measurements have some sensitivity to such layers," --> if you show the MAX-DOAS AVK, you can quantify/refer to its sensitivity in those layers

- Although the MAX-DOAS NO<sub>2</sub> averaging kernels show some sensitivity to altitudes as high as 1.5 km at times, we cannot confidently state that this retrieval always has sensitivity to the lower free troposphere since the PBL is changing throughout the day. Therefore, we have changed this sentence to the following on lines 845–846:  
*...do not account for free tropospheric NO<sub>2</sub> sources while the a priori NO<sub>2</sub> profile contains free tropospheric NO<sub>2</sub>.*

- line 593: "it is worthwhile to note that discrepancies between HeiPro and GEM-MACH profiles can be explained by the model inventories, " --> "can PROBABLY be explained by the.." (you don't show it is the case, you only assume it, right?!)

- We have now added “probably” to all sentences mentioning the GEM-MACH inventory as a plausible explanation for the bias (line 843 and line 955).

- line 598: "the smoothed GEM-MACH profile shows better agreement with HeiPro as it accounts for the MAX-DOAS measurement limitations and vertical sensitivity." --> please give also estimations for this case.

- Please see the [response above](#) as this point was also mentioned earlier.

- line 700: "partial column RMS fitting residuals": what are those RMS? RMS between measured and modelled dDSCD in the OE inversion? please explain. DOFs are also never really explained, it is taken as granted that the reader know what they are...

- Thank-you for flagging this. As mentioned in an above point, what was plotted was the retrieved NO<sub>2</sub> partial column error. This has been corrected in Figure A1 as well as any referencing text.
- Regarding the DOFS, we provide some more information in the manuscript on lines 314–315:

*...the degrees of freedom for signal (DOFS) for each profile, which represents the number of independent pieces of information obtained from the measurements...*

## References

Brion, J., Chakir, A., Daumont, D., Malicet, J., and Parisse, C.: High-resolution laboratory absorption cross section of O<sub>3</sub>. Temperature effect, *Chem. Phys. Lett.*, 213, 610–612, [https://doi.org/10.1016/0009-2614\(93\)89169-I](https://doi.org/10.1016/0009-2614(93)89169-I), 1993.

Brion, J., Chakir, A., Charbonnier, J., Daumont, D., Parisse, C., and Malicet, J.: Absorption Spectra Measurements for the Ozone Molecule in the 350–830 nm Region, *J. Atmos. Chem.*, 30, 291–299, <https://doi.org/10.1023/a:1006036924364>, 1998.

Cede, A.: Manual for Blick Software Suite 1.8, available at: [https://www.pandonia-global-network.org/wpcontent/uploads/2021/09/BlickSoftwareSuite\\_Manual\\_v1-8-4.pdf](https://www.pandonia-global-network.org/wpcontent/uploads/2021/09/BlickSoftwareSuite_Manual_v1-8-4.pdf), last accessed: 16 April 2024.

Chan, K. L., Wiegner, M., Wenig, M., and Pöhler, D.: Observations of tropospheric aerosols and NO<sub>2</sub> in Hong Kong over 5 years using ground based MAX-DOAS, *Science of The Total Environment*, 619–620, 1545–1556, <https://doi.org/10.1016/j.scitotenv.2017.10.153>, 2018.

Choi, S., Lamsal, L. N., Follette-Cook, M., Joiner, J., Krotkov, N. A., Swartz, W. H., Pickering, K. E., Loughner, C. P., Appel, W., Pfister, G., Saide, P. E., Cohen, R. C., Weinheimer, A. J., and Herman, J. R.: Assessment of NO<sub>2</sub> observations during DISCOVER-AQ and KORUS-AQ field campaigns, *Atmos. Meas. Tech.*, 13, 2523–2546, <https://doi.org/10.5194/amt-13-2523-2020>, 2020.

Daumont, D., Brion, J., Charbonnier, J., and Malicet, J.: Ozone UV spectroscopy I: Absorption cross-sections at room temperature, *J. Atmos. Chem.*, 15, 145–155, <https://doi.org/10.1007/bf00053756>, 1992.

Eskes, H. J. and Eichmann, K.-U.: S5P Mission Performance Centre Nitrogen Dioxide [L2 NO<sub>2</sub>] Readme, 2019.

Fleischmann, O. C., Hartmann, M., Burrows, J. P., and Orphal, J.: New ultraviolet absorption cross-sections of BrO at atmospheric temperatures measured by time-windowing Fourier transform spectroscopy, *J. Photoch. Photobio. A*, 168, 117–132, <https://doi.org/10.1016/j.jphotochem.2004.03.026>, 2004.

Herman, J., Cede, A., Spinei, E., Mount, G., Tzortziou, M., and Abuhassan, N.: NO<sub>2</sub> column amounts from ground-based Pandora and MFDOAS spectrometers using the direct-sun DOAS technique: Intercomparisons and application to OMI validation, *J. Geophys. Res.*, 114, D13307, <https://doi.org/10.1029/2009JD011848>, 2009.

Herman, J., Spinei, E., Fried, A., Kim, J., Kim, J., Kim, W., Cede, A., Abuhassan, N., and Segal-Rozenhaimer, M.: NO<sub>2</sub> and HCHO measurements in Korea from 2012 to 2016 from Pandora spectrometer instruments compared with OMI retrievals and with aircraft measurements during



the KORUS-AQ campaign, *Atmos. Meas. Tech.*, **11**, 4583–4603, <https://doi.org/10.5194/amt-11-4583-2018>, 2018.

Kreher, K., Van Roozendaal, M., Hendrick, F., Apituley, A., Dimitropoulou, E., Frieß, U., Richter, A., Wagner, T., Lampel, J., Abuhassan, N., Ang, L., Anguas, M., Bais, A., Benavent, N., Bösch, T., Bogner, K., Borovski, A., Bruchkouski, I., Cede, A., Chan, K. L., Donner, S., Drosoglou, T., Fayt, C., Finkenzeller, H., Garcia-Nieto, D., Gielen, C., Gómez-Martín, L., Hao, N., Henzing, B., Herman, J. R., Hermans, C., Hoque, S., Irie, H., Jin, J., Johnston, P., Khayyam Butt, J., Khokhar, F., Koenig, T. K., Kuhn, J., Kumar, V., Liu, C., Ma, J., Merlaud, A., Mishra, A. K., Müller, M., Navarro-Comas, M., Ostendorf, M., Pazmino, A., Peters, E., Pinardi, G., Pinharanda, M., Piders, A., Platt, U., Postlyakov, O., Prados-Roman, C., Puentedura, O., Querel, R., Saiz-Lopez, A., Schönhardt, A., Schreier, S. F., Seyler, A., Sinha, V., Spinei, E., Strong, K., Tack, F., Tian, X., Tiefengraber, M., Tirpitz, J.-L., van Gent, J., Volkamer, R., Vrekoussis, M., Wang, S., Wang, Z., Wenig, M., Wittrock, F., Xie, P. H., Xu, J., Yela, M., Zhang, C., and Zhao, X.: Intercomparison of NO<sub>2</sub>, O<sub>4</sub>, O<sub>3</sub> and HCHO slant column measurements by MAX-DOAS and zenith-sky UV–visible spectrometers during CINDI-2, *Atmos. Meas. Tech.*, **13**, 2169–2208, <https://doi.org/10.5194/amt-13-2169-2020>, 2020.

Krotkov, N. A., Lamsal, L. N., Celarier, E. A., Swartz, W. H., Marchenko, S. V., Bucsela, E. J., Chan, K. L., Wenig, M., and Zara, M.: The version 3 OMI NO<sub>2</sub> standard product, *Atmos. Meas. Tech.*, **10**, 3133–3149, <https://doi.org/10.5194/amt-10-3133-2017>, 2017.

Lin, J.-T. and McElroy, M. B.: Impacts of boundary layer mixing on pollutant vertical profiles in the lower troposphere: Implications to satellite remote sensing, *Atmospheric Environment*, **44**, 1726–1739, <https://doi.org/10.1016/j.atmosenv.2010.02.009>, 2010.

Meller, R. and Moortgat, G. K.: Temperature dependence of the absorption cross sections of formaldehyde between 223 and 323 K in the wavelength range 225–375 nm, *J. Geophys. Res.*, **105**, 7089–7101, <https://doi.org/10.1029/1999JD901074>, 2000.

Meng, K., Xu, X., Cheng, X., Xu, X., Qu, X., Zhu, W., Ma, C., Yang, Y., and Zhao, Y.: Spatio-temporal variations in SO<sub>2</sub> and NO<sub>2</sub> emissions caused by heating over the Beijing-Tianjin-Hebei Region constrained by an adaptive nudging method with OMI data, *Science of The Total Environment*, **642**, 543–552, <https://doi.org/10.1016/j.scitotenv.2018.06.021>, 2018.

Ortega, I., Koenig, T., Sinreich, R., Thomson, D., and Volkamer, R.: The CU 2-D-MAX-DOAS instrument – Part 1: Retrieval of 3-D distributions of NO<sub>2</sub> and azimuth-dependent OVOC ratios, *Atmos. Meas. Tech.*, **8**, 2371–2395, <https://doi.org/10.5194/amt-8-2371-2015>, 2015.

Rothman, L., Gordon, I., Barber, R., Dothe, H., Gamache, R., Goldman, A., Perevalov, V., Tashkun, S., and Tennyson, J.: HITEMP, the high-temperature molecular spectroscopic database, *J. Quant. Spectrosc. Ra.*, **111**, 2139–2150, <https://doi.org/10.1016/j.jqsrt.2010.05.001>, 2010.

Schreier, S. F., Richter, A., and Burrows, J. P.: Near-surface and path-averaged mixing ratios of NO<sub>2</sub> derived from car DOAS zenith-sky and tower DOAS off-axis measurements in Vienna: a case study, *Atmos. Chem. Phys.*, **19**, 5853–5879, <https://doi.org/10.5194/acp-19-5853-2019>, 2019.

Serdyuchenko, A., Gorshelev, V., Weber, M., Chehade, W., and Burrows, J. P.: High spectral resolution ozone absorption crosssections – Part 2: Temperature dependence, *Atmos. Meas. Tech.*, 7, 625–636, <https://doi.org/10.5194/amt-7-625-2014>, 2014.

Thalman, R. and Volkamer, R.: Temperature dependent absorption cross-sections of O<sub>2</sub>–O<sub>2</sub> collision pairs between 340 and 630 nm and at atmospherically relevant pressure, *Phys. Chem. Chem. Phys.*, 15, 15371–15381, <https://doi.org/10.1039/C3CP50968K>, 2013.

Thermo Scientific. (2015). Model 42i instruction manual: Chemiluminescence NO-NO<sub>2</sub>-NO<sub>x</sub> analyzer (Part No. 101350-00, 25JUL2015). Thermo Fisher Scientific.

Vandaele, A., Hermans, C., Simon, P., Carleer, M., Colin, R., Fally, S., Mérienne, M., Jenouvrier, A., and Coquart, B.: Measurements of the NO<sub>2</sub> absorption cross-section from 42 000 cm<sup>-1</sup> to 10 000 cm<sup>-1</sup> (238–1000 nm) at 220 K and 294 K, *J. Quant. Spectrosc. Ra.*, 59, 171–184, [https://doi.org/10.1016/S0022-4073\(97\)00168-4](https://doi.org/10.1016/S0022-4073(97)00168-4), 1998.

Vlemmix, T., Hendrick, F., Pinardi, G., De Smedt, I., Fayt, C., Hermans, C., PETERS, A., Wang, P., Levelt, P., and Van Roozendaal, M.: MAX-DOAS observations of aerosols, formaldehyde and nitrogen dioxide in the Beijing area: comparison of two profile retrieval approaches, *Atmos. Meas. Tech.*, 8, 941–963, <https://doi.org/10.5194/amt-8-941-2015>, 2015.

York, D., Evensen, N. M., Martínez, M. L., and De Basabe Delgado, J.: Unified equations for the slope, intercept, and standard errors of the best straight line, *American Journal of Physics*, 72, 367–375, <https://doi.org/10.1119/1.1632486>, 2004.

Zhao, X., Griffin, D., Fioletov, V., McLinden, C., Davies, J., Ogyu, A., Lee, S. C., Lupu, A., Moran, M. D., Cede, A., Tiefengraber, M., and Müller, M.: Retrieval of total column and surface NO<sub>2</sub> from Pandora zenith-sky measurements, *Atmos. Chem. Phys.*, 19, 10619–10642, <https://doi.org/10.5194/acp-19-10619-2019>, 2019.

Zhao, X., Griffin, D., Fioletov, V., McLinden, C., Cede, A., Tiefengraber, M., Müller, M., Bognar, K., Strong, K., Boersma, F., Eskes, H., Davies, J., Ogyu, A., and Lee, S. C.: Assessment of the quality of TROPOMI high-spatial-resolution NO<sub>2</sub> data products in the Greater Toronto Area, *Atmos. Meas. Tech.*, 13, 2131–2159, <https://doi.org/10.5194/amt-13-2131-2020>, 2020.

Zhao, X., Fioletov, V., Alwarda, R., Su, Y., Griffin, D., Weaver, D., Strong, K., Cede, A., Hanisco, T., Tiefengraber, M., McLinden, C., Eskes, H., Davies, J., Ogyu, A., Sit, R., Abboud, I., and Lee, S. C.: Tropospheric and Surface Nitrogen Dioxide Changes in the Greater Toronto Area during the First Two Years of the COVID-19 Pandemic, *Remote Sensing*, 14, 1625, <https://doi.org/10.3390/rs14071625>, 2022.